Glangeaud L., Aymé A., Mattauer M., and Muraour P., 1952, Histoire géologique de la province d'Alger. XIXème Congrès Géologique International, Monographies Régionales, 1ère Série, Algérie, N. 25

Hanks and Kanamori, 1979, A moment magnitude scale, J.G.R., 84, 2348-2350.

Idriss, 1985, Proceed. 11th Conf. Soil Mech. & Found. Eng., San Francisco, V1, Bolkema Ed. 255-330.

Kanamori, 1977, The energy release in great earthquakes, J.G.R., 82, 2981-2987.

Maouche S., 2000, Etude sismotectonique de l'Algérois et des zones limitrophes de Cherchell-Gouraya. Thèse de Magister, Université des Sciences et de la Technologie Houari Boumediene, Bâb Ezzouar, Alger, Algérie, 130 pp.

Meghraoui M., 1991, Blind reverse faulting system associated with the Mount Chenoua-Tipaza earthquake of 29 octobre 1989, (North-Central Algeria), Terra Nova, 3, 84-93.

Saadallah A., 1981, Le massif cristallophyllien d'El-Djazaïr (Algérie): évolution d'un charriage à vergence nord dans les Internides des Maghrébides. Thèse de Doctorat, Université des Sciences et de la Technologie Houari Boumédiene, 160 pages.

Saadallah, 1984, Tectonique globale et active en Algérie alpine septentrionale: facteurs determinants pour une approche de la définition de l'aléa sismique. Conférence Internationale sur la Microzonation sismique, Actes de la Conférence, Tome II, pp. 121-135.

Saoudi N., 1989, Pliocène et Pléistocène inférieur et moyen du Sahel occidental d'Alger. Entreprise National du Livre, Alger, 1989.

Slemmons D. and Lugaski T., 1984, Preliminary evaluation of maximum earthquakes, Algiers region, Algeria. Conférence Internationale sur la Microzonation sismique, Actes de la Conférence, Tome II, pp. 143-152.

Swan et al., 1998, Probabilistic seismic hazard assessment of the Algiers region. Geomatrix Consultant report.

Wells D.L., & Coppersmith K.J., 1994, New empirical relationships among Magnitude, Rupture Length, Rupture Width, Rupture Area and Surface Displacement. Bulletin of the Seismological Society of America, 84, pp. 974-1002.

Yelles K., Lammali K., and Mahsas A., 2004, Coseismic deformation of the May 21st, 2003, Mw=6.8 Boumerdes earthquake, Algeria, from GPS measurements. Geophysical Research Letters, v. 31, L13610, doi:10.1029/2004GL019884.

Youngs R. R. and Coppersmith K. J., 1985, Implications of fault slip rates and earthquake recurrence models to probabilistic seismic hazard estimates, Bull. Seism. Soc. Am. 75, 939-964.

5-2 Ground Modeling

Earthquake motion at the ground surface is strongly affected by subsurface soil structure. The effects of soils on seismic motion are evaluated by numerical simulation. For this purpose, the surface ground models of each 250 m grid were made based on geological, geotechnical and geophysical information. These ground models are also used in liquefaction potential analysis. The ground modeling was conducted following the flow in Figure 5-9.

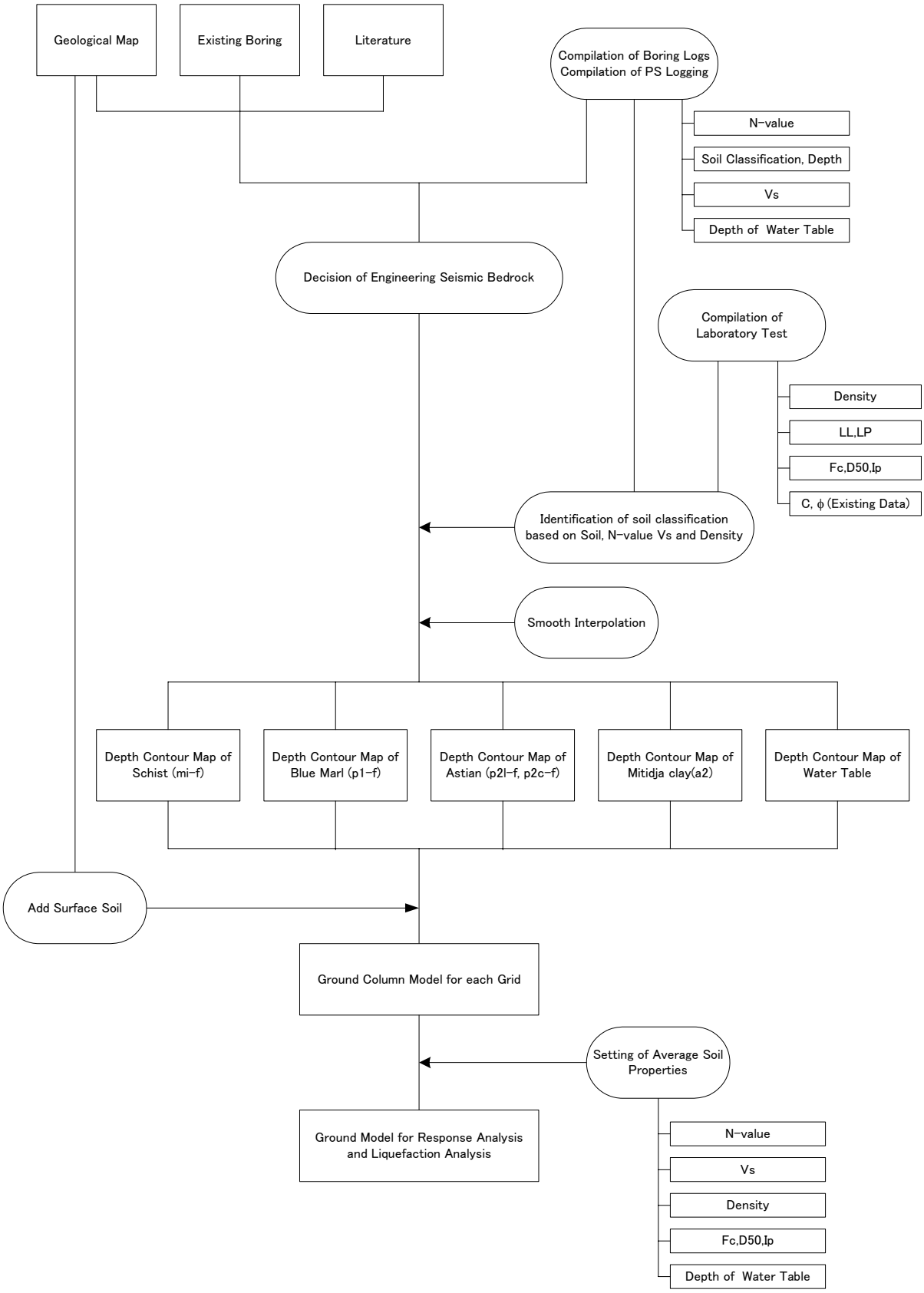

Figure 5-9 Flowchart of Ground Modeling

(1) Compilation of Boring Logs and PS Logging

The boring logs and PS loggings conducted in this study were compiled with existing boring data. The boring and PS logging data is presented in Section 3-3-1 and Section 3-3-3 in detail. The compilation was conducted mainly for the following parameters;

- N-value by SPT (Standard Penetration Test)
- Soil classification and depth of the boundaries of soil layers
- S wave velocity (Vs)
- Depth of ground water table

In the compilation, the location and elevation of each boring point are also very important information. The newly conducted boring location was measured by the boring contractor and checked by GPS measurement and DEM (Digital Elevation Model).

(2) Determination of Engineering Seismic Bedrock

The earthquake motion was determined by separately calculating earthquake motion for seismic bedrock and evaluating subsurface layer amplification over bedrock. This is due to the necessity to deal differently with subsurface amplification from the calculation for seismic bedrock since characteristics of the former vary widely with soil properties near the ground surface.

In general, seismic bedrock may be defined as follows:

- It is distributed over the entire survey region
- Fluctuations in physical properties below this layer are smaller than those in the layers above
- Vs = 3.0 km/sec or more.

Actually, seismic bedrock with Vs of 3.0 km/sec or more sometimes extends to a depth of several kilometers within the sedimentary basin and a large-scale geophysical survey is necessary to understand its structure. Because the distribution of the seismic bedrock around the study area is unknown, “engineering” seismic bedrock was used instead.

Depending on the existing geological map, existing boring, literature and compiled boring logs and PS loggings, fresh Plaisancian blue marl (p1-f) with Vs of 630 m/sec was adopted as “engineering” seismic bedrock. This Plaisancian blue marl can be found over almost the entire study area except for the north-west part, e.g. BAB EL OUED and BOUZAREAH, and the north-east end, e.g. EL MARSA. In these areas, sediments or weathered rock directly cover the schist (mi-f) and this schist layer, with a Vs of 1030 m/sec, was used for the engineering seismic bedrock in these areas. The distribution of the aforementioned engineering seismic bedrock is shown in Figure 5-10.

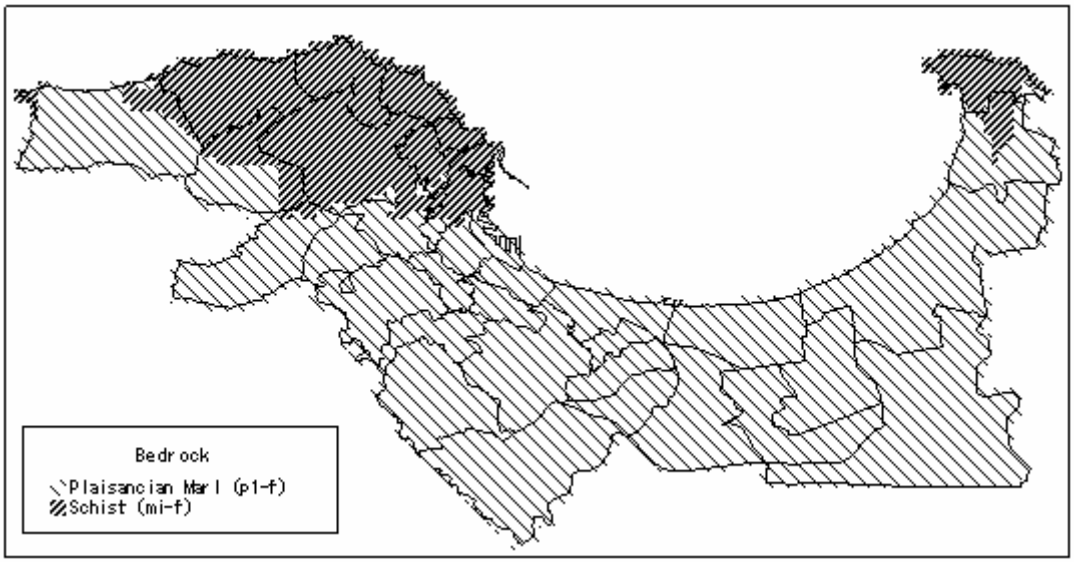

Figure 5-10 Distribution of Two Kinds of Engineering Seismic Bedrock

(3) Compilation of Laboratory Tests

The laboratory test data conducted in this study were compiled with collected existing data. The data are shown in Section 3-3-2. The compilation was conducted mainly for the following parameters;

- Density
- Atterberg's limit (LL, LP)
- Fine fraction content (Fc)
- Grain diameter of 50% passing (D50)
- Plasticity index (Ip)
- Cohesion (C) and Friction angle (ϕ) (only existing data)

(4) Identification of Soil Classification

Based on the compiled boring data, PS logging data and laboratory test data, the soils identified in the Study Area were classified for the purpose of engineering geology. The classification of soils is shown in Table 5-4. The soil layer in each boring log was classified according to this classification.

Table 5-4 Classification of Soils for Engineering Geology

Symbol	Explanation
ap	Beach deposit and dune deposit
e	Slope deposit
a3	Quarternary deposit (sand)
a2	Quarternary deposit (clay)
q	Old Quarternary deposit
qt	Marine terrace
p2c	Astian layer (marl, weathered)
p2c-f	Astian layer (marl, fresh)
p2l	Astian calcareous layer (weathered)
p2l-f	Astian calcareous layer (fresh)
p1	Plaisancian layer (blue marl, weathered)
p1-f	Plaisancian layer (blue marl, fresh)
mi	Metamorphic rocks (schist, weathered)
mi-f	Metamorphic rocks (schist, fresh)

(5) Smooth Interpolation

The depth of soil layers was identified at 50 new drilled boring points and at several existing boring points. Schist, Plaisancian layer and

Astian layer show a gentle inclination in the study area from the boring logs and literature, therefore, the depth of these layers at each 250 m grid was estimated with numerical interpolation techniques using these limited points of data. The "surface analysis" function of ArcGIS was used for this purpose. Because this numerical interpolation sometimes shows unrealistic depth distribution due to lack of data or unavoidable error in the data, the depth distribution was revised based on the following rule.

- Older deposits don't cover younger layers.
- Ground surface is covered by weathered rock or soil.

The depth of schist (mi-f), blue marl (p1-f), Astian layers (p2l-f, p2c-f) and Mitidja clay (a2) are shown in Figure 5-11.

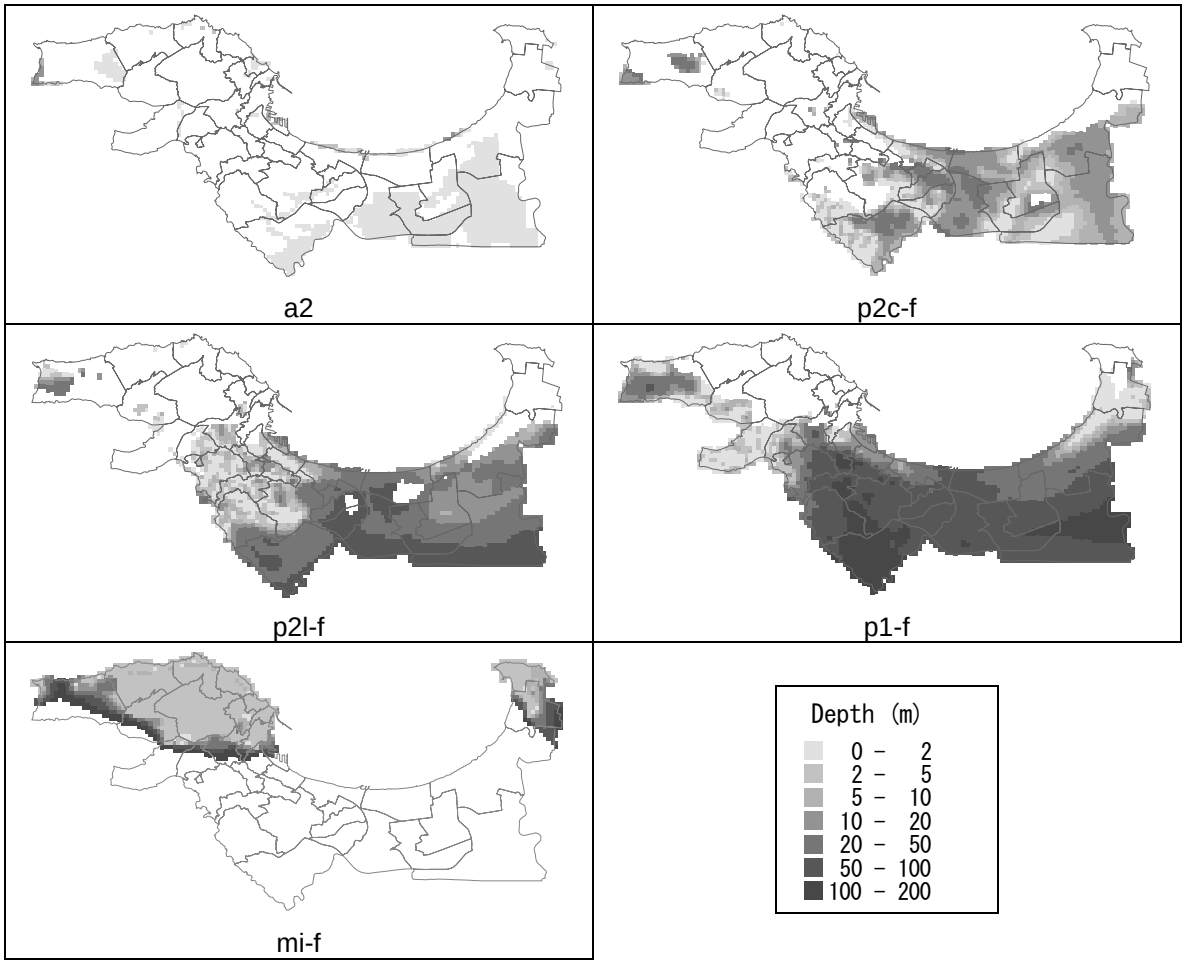

Figure 5-11 Interpolated Depth of Layers

(6) Surface Soil

Unlike the rock and hard soils, the soft surface soil usually shows obvious locality. The surface soils shallower than the Astian layer may show a big difference within a short distance. The boring density was not adequate to estimate the surface soil properties. Hence the geological map (Figure 3-19) was used to estimate surface soil condition at each 250 m grid . Figure 5-12 shows the surface soil distribution.

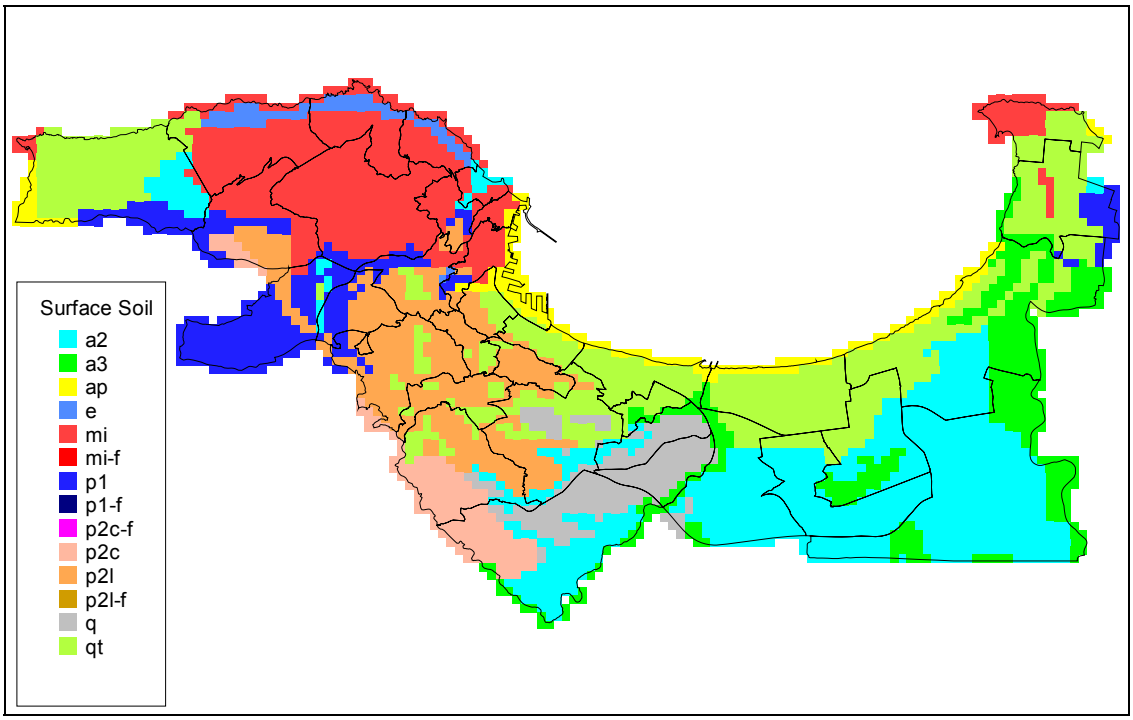

Figure 5-12 Surface Soil

(7) Setting of Average Soil Properties

The following geotechnical and geophysical parameters were set for each layer of the 250 m grid model based on the parameters in Table 3-16.

1) For response analysis

- Depth
- Vs
- Density

2) For liquefaction analysis

- Depth
- N-value (depth dependency is considered, see section 5-4)
- Fc
- D50
- p
- Water level

Figure 5-13 and Figure 5-14 show typical sections of the ground in an east-west direction and north-south direction in the Study Area respectively. Figure 5-15 shows an example of the geological model.

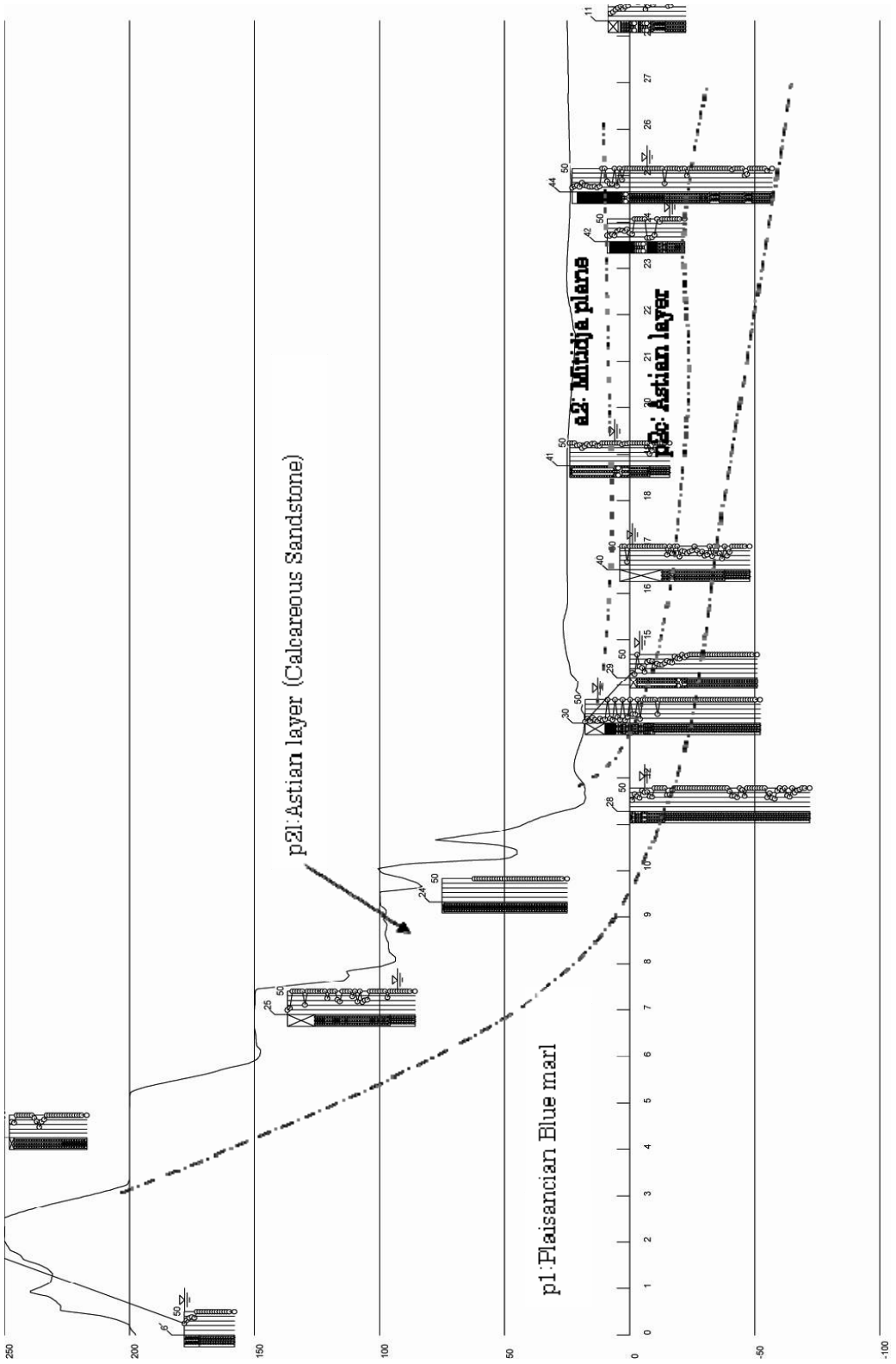

Figure 5-13 Typical Cross Section of the Study Area (east-west (Boring No. 6-Boring No. 11))

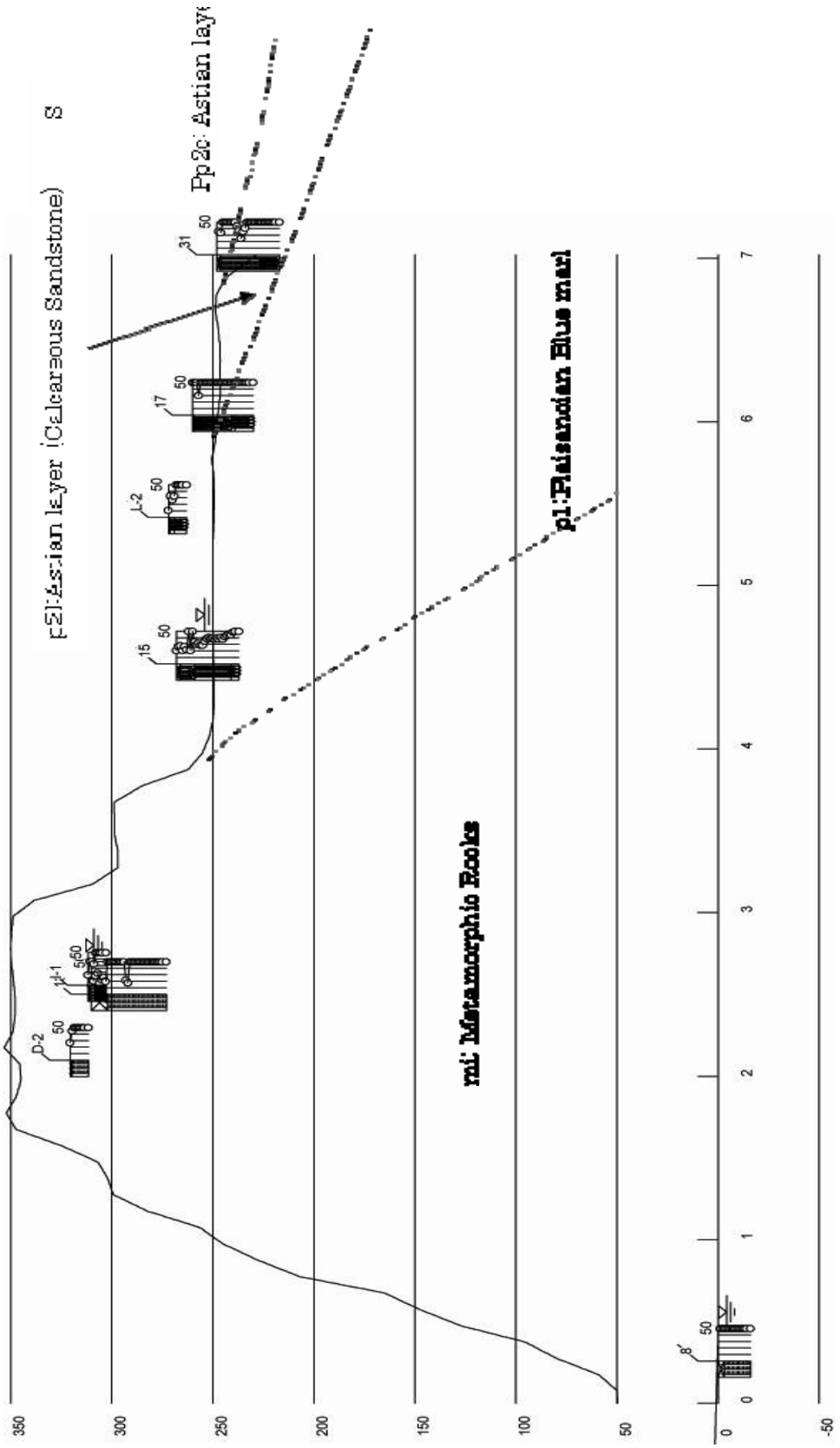

Figure 5-14 Typical Cross Section of the Study Area (north-south (Borehole No. 8-Borehole No. 31))

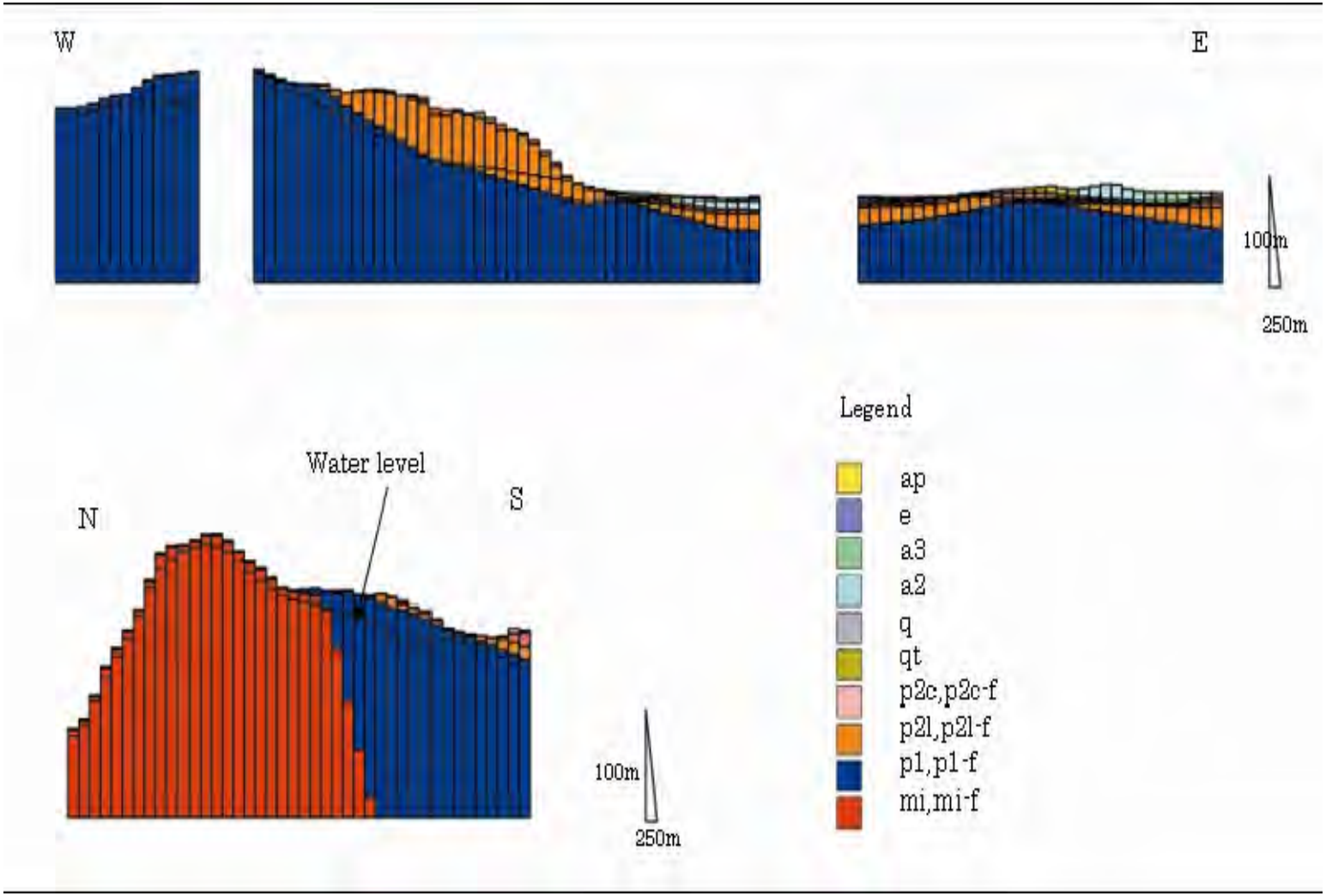

Above chart: The same section as Figure 5-14
Below chart: The same section as Figure 5-14

Figure 5-15 Ground Model Converted from Typical Model

5-3 Estimation of Ground Motion

5-3-1 Bedrock Motion Analysis

Effects produced by the seismogenic sources are quantified through parameters of ground motion (acceleration, velocity, spectral acceleration, etc.). These effects are calculated using attenuation laws based on source-to-site distances, magnitude and depth of hypocenter. The attenuation laws are chosen according to the seismotectonic context and comparison with the observed strong motion records and the bedrock motion is provided as a map of ground motion for a given return period. These are provided in this report as maps of horizontal Peak Ground Accelerations (PGAs) at bedrock for a 475 year return period (i.e. 10% probability of exceedance within 50 years).

(1) Attenuation Relationships

Horizontal Peak Ground Accelerations at bedrock, associated with reference earthquakes, are calculated using appropriate attenuation relationships. Initially, the following three attenuation relationships were selected after considering Algerian records:

- Laouami et al. (2005): Empirical relationship developed by Laouami et al. (2005) allows calculation of horizontal PGA for earthquakes with surface magnitude (Ms) ranging from 5.7 to 6.0, for hypocentral distances ranging from 13 to 70 km. This attenuation law considers neither type of ground nor style of faulting and is based on the four Algerian earthquakes.
- Ambraseys et al. (2005): Empirical relationship developed by Ambraseys et al. (2005) allows calculation of horizontal PGA and response spectra for earthquakes for which moment magnitude (Mw) ranges between 5.0 and 7.6, for distances to the surface projection of the fault ranging between 0 and 100 km, and for shallow earthquakes. These relationships take into account the type of soil (rock/firm soil/soft soil), with $Vs_{,30}$ > 750 m/s for rock type, and the mechanism of deformation (reverse/strike-slip/normal). The equations are based on data from Europe and the Middle-East, including 15 records from Algeria.
- Berge-Thierry et al. (2003): Empirical relationship developed by Berge-Thierry et al. (2003) allows calculation of horizontal PGA and response spectra for earthquakes for which surface magnitude (Ms) ranges between 4.0 and 7.9, focal distance ranges between 4 and 330 km, and for shallow earthquakes. These relationships take into account the type of soil (rock/soil) with $Vs_{,30}$ > 800 m/s for rock type. The equations are based on data from Europe, California and the Middle-East, including 3 records from Algeria.

The applicability of these three attenuation relationships to Algiers area was evaluated through comparison with the strong motion records observed in the 2003 Boumerdes earthquake. Figure 5-16 shows the strong motion observatory that recorded the Boumerdes earthquake along with the epicenter and the seismic source fault by Delouis et al. (2004). The PGA values of horizontal components are plotted in Figure 5-17 according to the ground condition. The acceleration value at the bedrock of the HUSSEIN DEY and KOUBA observatory are analysed by response analysis (SHAKE) based on the newly conducted PS-logging results at exact points. These values, plotted on Figure 5-17, are around 40 km

epicentral distance or 25 km distance from the surface projection of the fault. The ground model of HUSSEIN DEY and KOUBA is shown in Table 5-5.

The lines in the upper graphs in Figure 5-17 are the formulae by Laoumi et al. (2005) and Berge-Thierry et al. (2003), while that of Ambraseys et al. (2005) is in the lower graphs. The formula by Ambraseys et al. (2005) provides better estimates than the other two. The main reason is that the method of Ambraseys et al. (2005) can evaluate the extent of seismic source while the others cannot. If the magnitude is small, the seismic source can be treated as a point source and the calculated values based on these three formulae will diff greatly. However, the magnitude of scenario earthquakes in this Study is not sufficiently small. Therefore we have decided to use the method of Ambraseys et al. (2005) for bedrock motion calculation in this Study.

The formula of Ambraseys et al. (2005) to calculate PGA is:

$$\log y = 2.522 - 0.142Mw + (-3.184 + 0.314Mw)\cdot \log\sqrt{d^2 + 7.6^2} + \begin{cases} 0.137 : \text{soft soil} \\ 0.050 : \text{stiff soil} \\ 0.0 \quad : \text{rock} \end{cases} + \begin{cases} 0.062 : \text{thrust} \\ 0.0 : \text{strike - slip} \end{cases}$$

y : PGA(m/sec^2)

Mw : moment magnitude

d : distance to the surface projection of the fault (km)

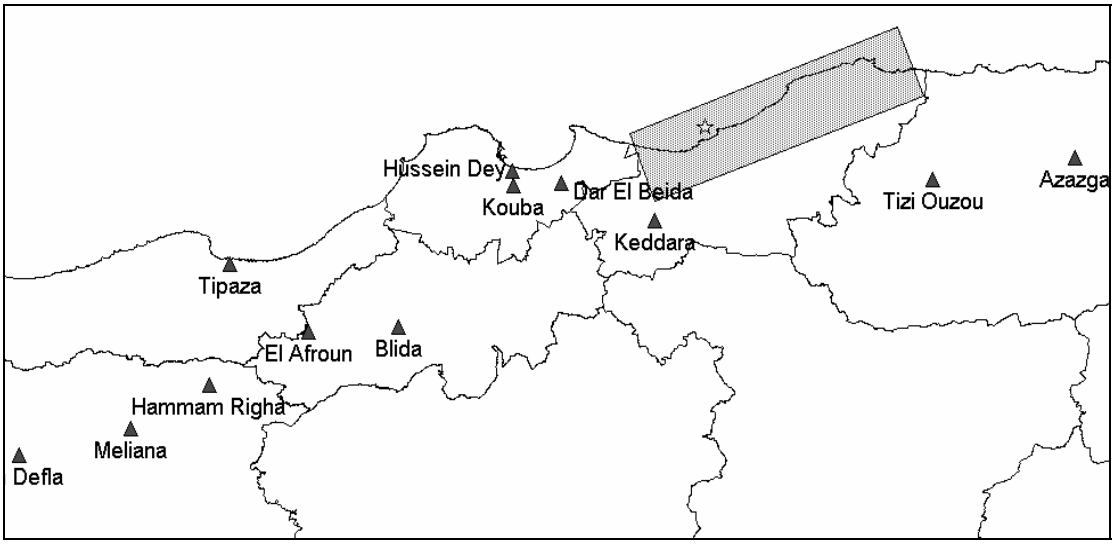

Figure 5-16 Location of Strong Motion Observatory that Recorded Boumerdes Earthquake; triangle: observatory, star: epicenter, rectangle: source fault by Delouis et al. (2004)

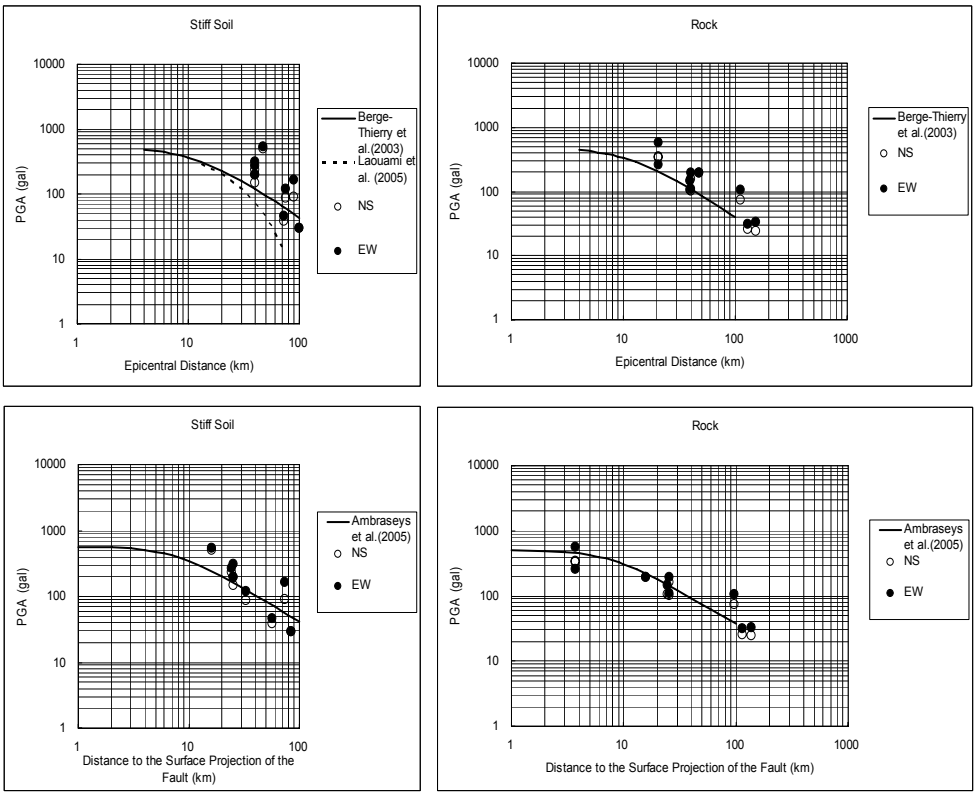

Figure 5-17 Comparison of Observed PGA with Attenuation Formula

Table 5-5 Ground Model for Response Analysis at Strong Motion Observatory

HUSSEIN DAY

Depth (m)	Soil	Vs (m/sec)	Density (g/cm^3)
0	Fill	200	1.8
2	Red Sand	300	1.85
7	Sand Stone	680	2.2
16	Blue Marl	470	1.8
20	Blue Marl	670	2.0
32	Blue Marl	520	1.9
58	Blue Marl	780	2.0

KOUBA

Depth (m)	Soil	Vs (m/sec)	Density (g/cm^3)
0	Fill	300	1.7
3	Sand Stone	380	1.9
11	Silt Stone/Sand Stone	480	1.9
40	Marl/Sand Stone	870	1.9

(2) Bedrock Motion

The source fault models of the six scenario earthquakes are shown in Figure 5-18. For each fault model, distances from each grid center to surface projection of source faults were measured and PGA at bedrock was calculated. According to the definition of Ambraseys et al. (2005), bedrock means the site with S-wave velocity more than 30 m from the surface exceeding 750 m/s.

The maps of PGA generated by a 475 year return period scenario earthquake are given in Figure 5-19. The map for Boumerdes earthquake is also given in Figure 5-19.

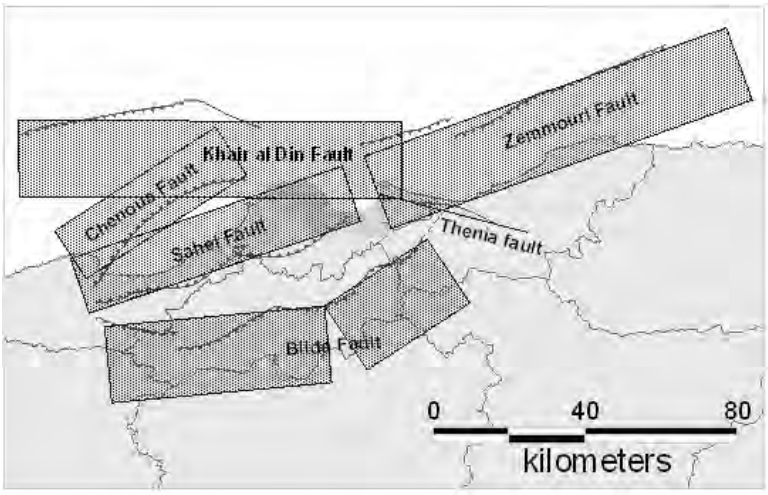

Figure 5-18 Fault Models of Scenario Earthquakes

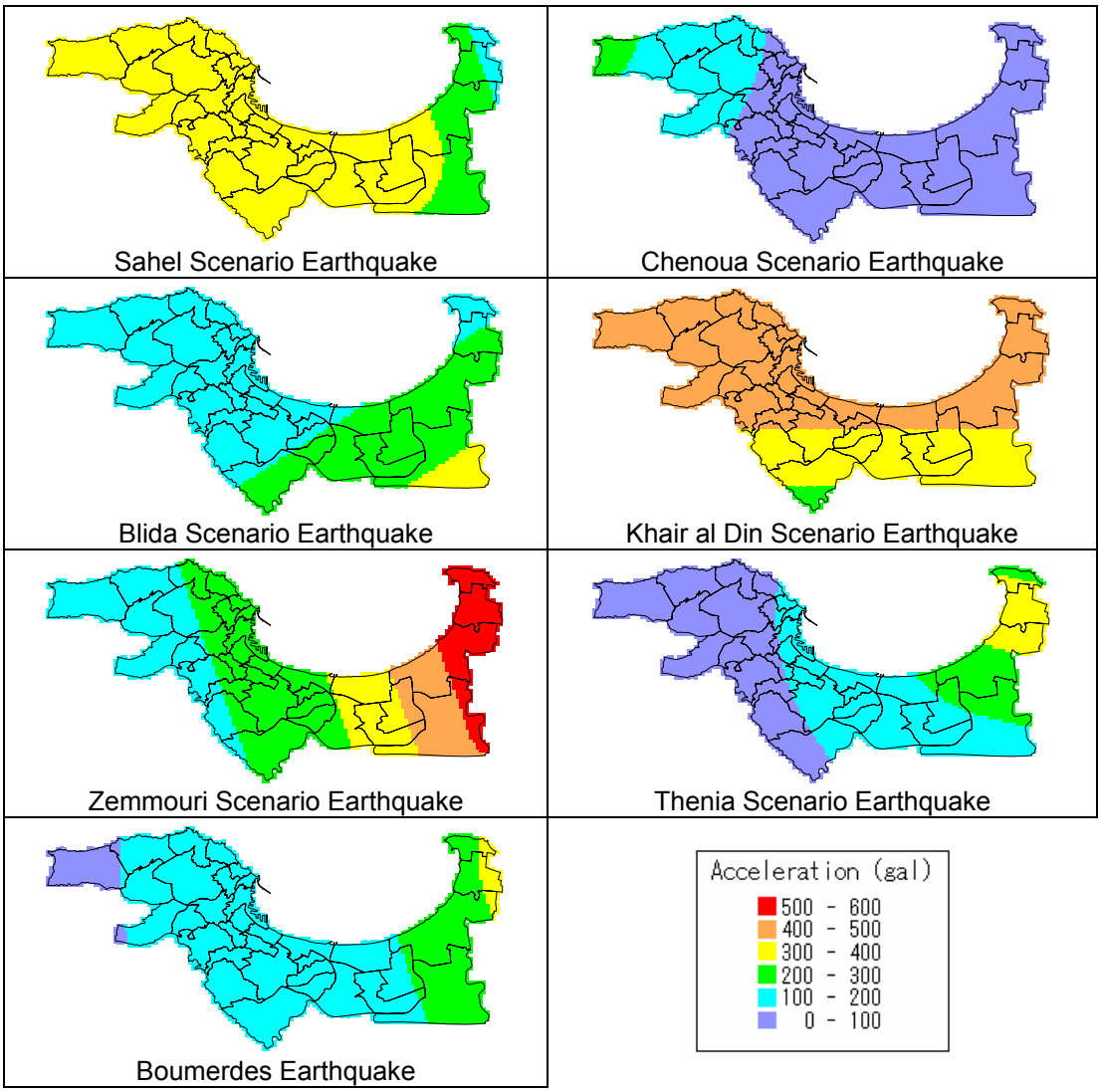

Figure 5-19 Acceleration Distribution at Bedrock

5-3-2 Subsurface Amplification Analysis

Earthquake motion at ground surface is strongly affected by subsurface soil structures, especially in the area covered by quaternary sediments. The effects of soils on seismic motion were evaluated by response analysis based on the 4013 ground models of each 250 m grid. The earthquake ground motion was provided as a map of PGA and seismic intensity distribution for six scenario earthquakes and for the 2003 Boumerdes earthquake.

The amplification of subsurface soil over engineering seismic bedrock was estimated by the 1D response analysis code SHAKE. This code analyses the propagation of shear wave through horizontally layered media over bedrock. The following settings or conditions were adopted in the analysis.

(1) Input motion

The bedrock motion calculated in Section 5-3-1 was defined assuming a layer of over 30 m from the surface has a Vs larger than 750 m/sec. Because the attenuation formula of Ambraseys et al. (2005) that was applied could evaluate bedrock motion at HUSSEIN DEY (Vs=780 m/sec) and KOUBA (Vs=870 m/sec) during the Boumerdes earthquake (see Section 5-3-1), the bedrock motion by Ambraseys et al. (2005) can be regarded to be on the layer of Vs=750 m/sec in the case of Algiers. As Vs of Plaisancian marl is 630 m/sec and schist is 1030 m/sec, the acceleration at seismic engineering bedrock was calculated using the following empirical relation of Vs and amplification by Midorikawa et al. (1994).

$$\log R = 1.35 - 0.47 \log V$$

R : amplification factor for PGA

V : average S - wave velocity to a depth of 30 m (m/sec)

(2) Non-linear property of soils

It is well known that soft soil layers show non-linear properties when seismic motion is sufficiently large. In proportion to the strain level, rigidity of the soil becomes low and damping ratio becomes high. This non-linear property affects the amplification of seismic motion if the covering soft soil layer is thick. As shown in Section 3-4, the average N-value of soils in Algiers exceeds 10 and S-wave velocity is more than 240 m/sec. Based on experience in Japan and other countries, the soil in Algiers is not too soft and it was assumed the non-linear effect of soil is not significant in amplification analysis.

In this Study, the response analysis was conducted both in linear and non-linear contexts to check the effect of the non-linear property. As there is no dynamic soil laboratory test to evaluate the non-linear dynamic property of soil in Algeria, the existing non-linear dynamic property of soil used in a seismic microzoning study of Tokyo Metropolitan Area, Japan, was applied after considering similarities of soil, S-wave velocity and N-value. The non-linearity of soils “ap”, “a3”, “e”, “a2” and “q” were considered and other soils were treated as linear material. Figure 5-20 shows the adopted non-linear properties of soils.

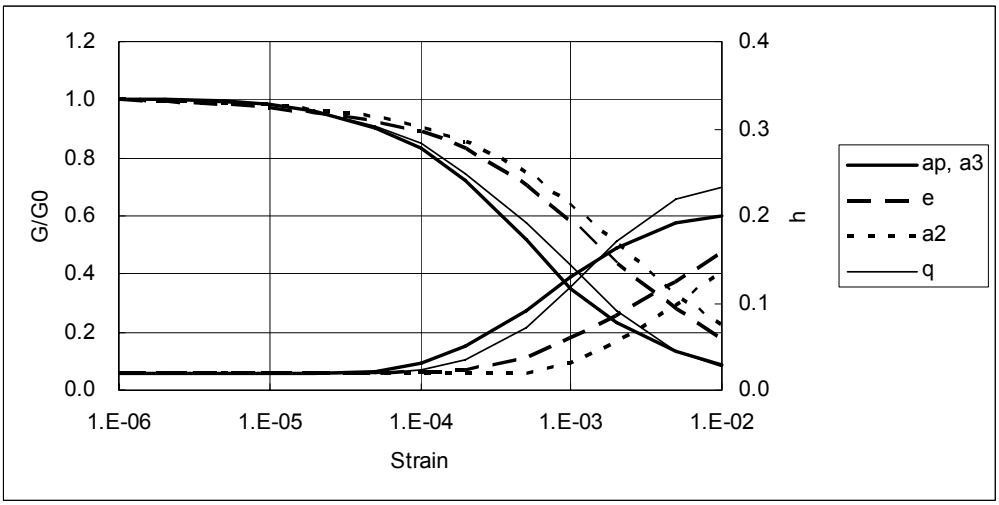

Figure 5-20 Non-linear Properties of Soils

(3) Input seismic waves

The amplification characteristics of subsurface layers differ depending on input seismic waves to the ground model. In this Study, the estimated bedrock waves during the 2003 Boumerdes earthquake were used as input motion. The magnitude of the Boumerdes earthquake, Mw=6.9, is comparable to the scenario earthquakes and the distance from source area to the Study Area also does not differ much. Therefore the frequency contents of the observed seismic waves in Algiers during the Boumerdes earthquake are suitable for input motion of the response analysis.

As shown in Section 5-3-1, the surface ground motion at HUSSEIN DEY and KOUBA strong motion station were de-amplified with response analysis and the bedrock waves estimated. The maximum amplitude of input waves was calibrated to the bedrock motion at each grid. Two horizontal components of each station were used; therefore four wave forms were used in the analysis. The wave forms of four input waves are shown in Figure 5-21. The averaged value of four calculated PGA values, which correspond to four input waves, was used as the final result.

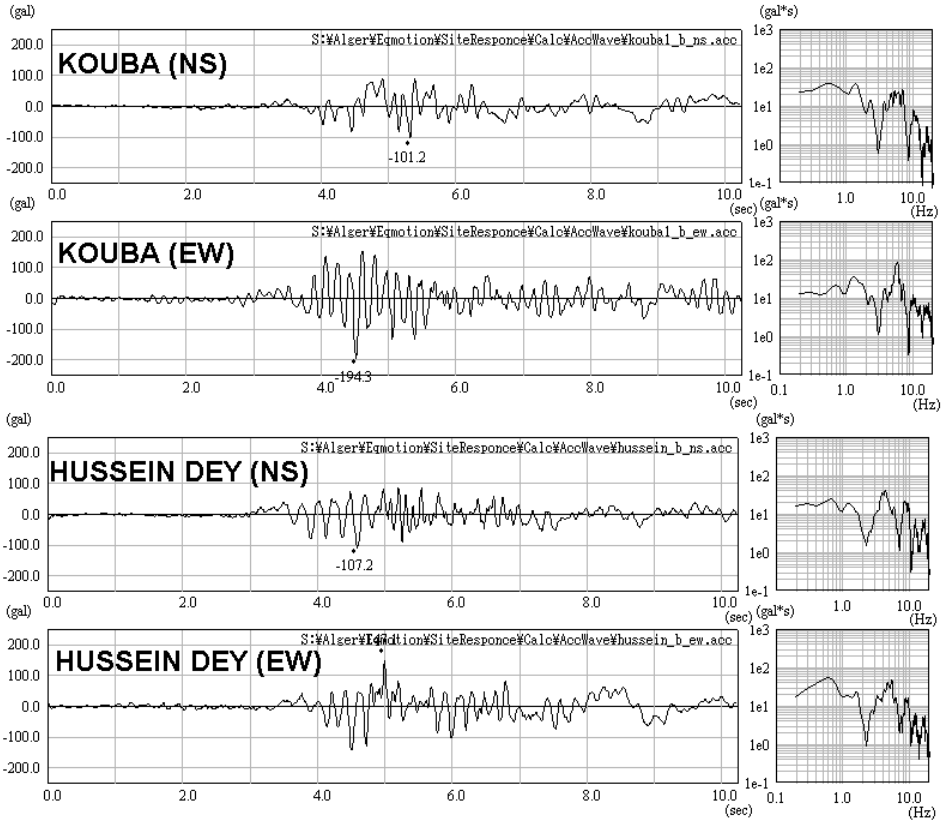

Figure 5-21 Used Input Waves for Response Analysis

5-3-3 Evaluation of Earthquake Ground Motion

The PGA value of ground surface at each grid was calculated from bedrock motion and response analysis.

(1) Peak Ground Acceleration (PGA)

The PGA distribution was estimated by non-linear and linear analysis. The results of linear analysis show slightly larger PGA in the eastern area, however, the difference is small. The results of non-linear analysis (Figure 5-22) are subsequently used as PGA distribution.

- Khair al Din scenario earthquake shows the largest PGA of almost all areas among the six scenario earthquakes except DAR EL BEIDA. Part of AIN BENIAN, BORDJ EL KIFFAN, DAR EL BEIDA and port area show more than 800 gal. Almost all the Study Area suffers more than 300 gal.
- DAR EL BEIDA experienced the largest PGA during the Zemmouri scenario earthquake, however, the PGA in the western half of the Study Area based on this scenario is lower by 300 gal.
- The PGA for the Sahel scenario earthquake is 300 gal greater, except for EL MARSA and BORDJ EL BAHRI. The PGA distribution pattern is similar to or smaller than that of Khair al Din scenario earthquake.

- Blida scenario earthquake and Thenia scenario earthquake result in more than 500 gal to the limited grid in the eastern part of the Study Area and less than 200 gal to the western part.
- The effect by the Chenoua scenario earthquake is limited to AIN BENIAN, with a PGA of up to 500 gal.
- The estimated PGA distribution of the Boumerdes earthquake shows around 200 gal at HUSSEIN DEY and KOUBA strong motion station, which is comparable to the observed PGA. The estimated PGA at DAR EL BEIDA strong motion station is around 400gal and smaller than the observed PGA of around 500 gal. This difference may be due to the local site effects or the setting of the strong motion seismometer.

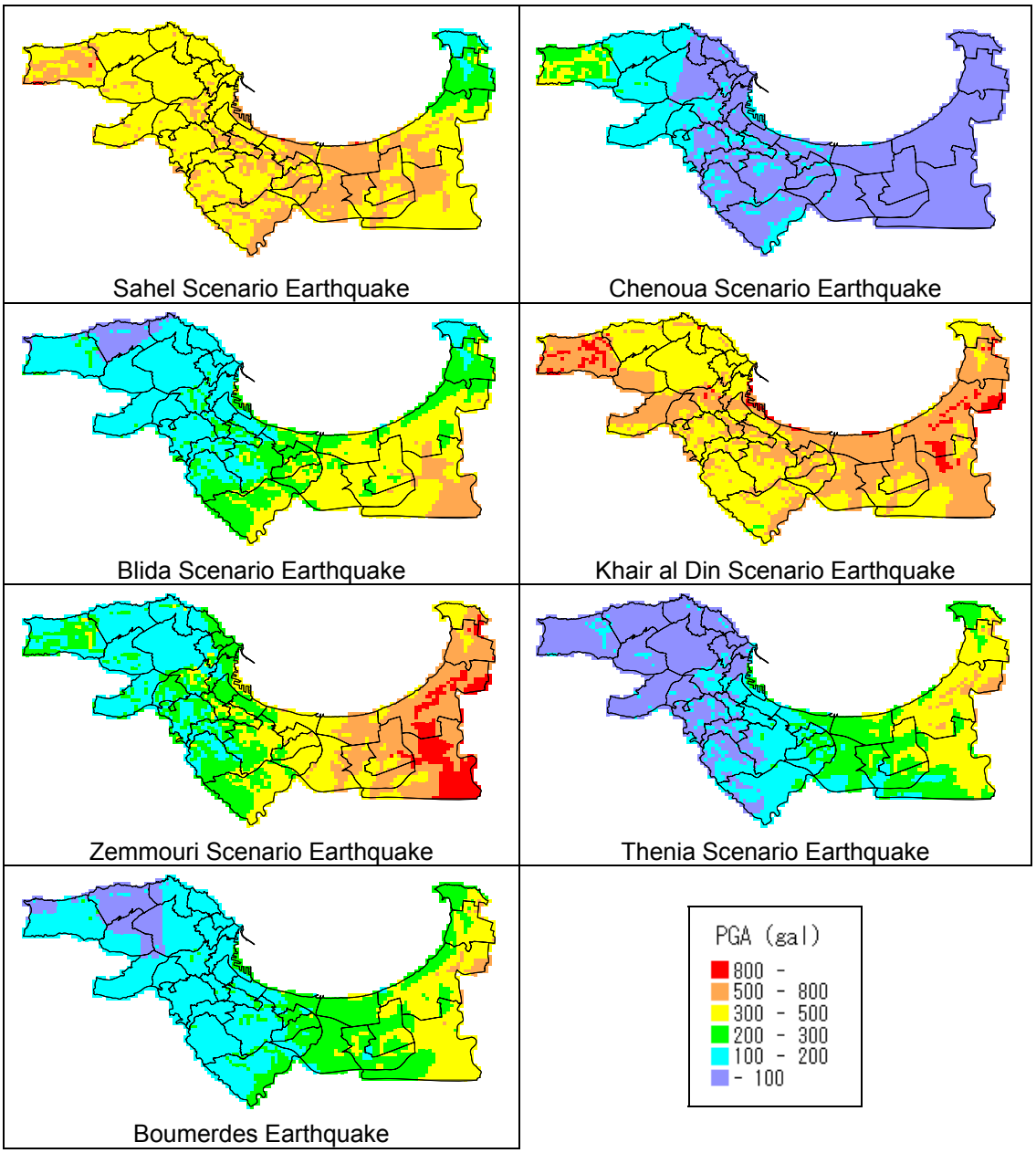

Figure 5-22 Peak Ground Acceleration Distribution at Ground Surface

(2) Seismic Intensity

The seismic intensity is basically determined from the feelings of humans or damage to the buildings and facilities. Therefore, seismic intensity cannot be directly calculated through numerical analysis. Though seismic intensity is not a physical value, it is a very important parameter for earthquake disaster prevention purposes. It is the only parameter when instrumental observations are not available.

Many researchers have proposed empirical relations between seismic intensity and physical parameters such as PGA or PGV. These show wide variability because of the difference of buildings, facilities and ground conditions of the data used in the analyses. In this Study, the seismic intensity in MSK scale and strong motion records by CGS during the 1989 Chenoua earthquake, 1999 Ain Timouchent earthquake and 2003 Boumerdes earthquake, were collected and the new relationship for Algeria was devised. Figure 5-23 is the relation between PGA and seismic intensity in MSK scale. The estimated seismic intensity distributions by this empirical relation are shown in Figure 5-24.

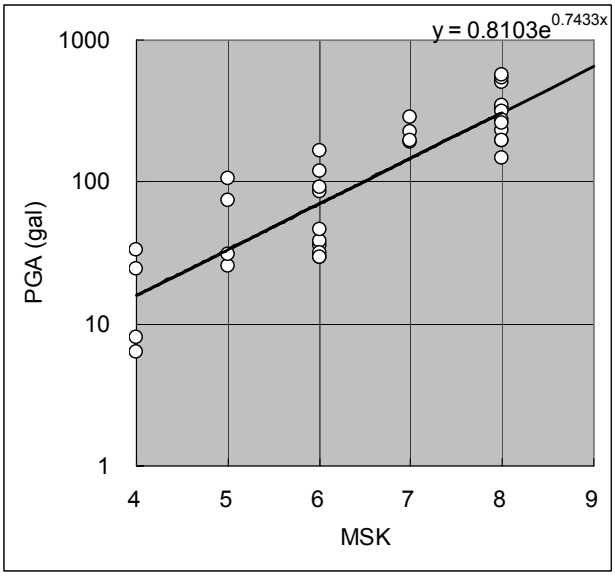

Figure 5-23 Empirical Relation between PGA and Seismic Intensity in MSK Scale

- Khair al Din scenario earthquake shows largest seismic intensity in almost all areas among the six scenario earthquakes except at DAR EL BEIDA. Part of AIN BENIAN, BORDJ EL KIFFAN, DAR EL BEIDA and the port area show an intensity of 10. All of the Study Area suffers an intensity exceeding 8.
- Some areas in DAR EL BEIDA experienced intensity 10 during the Zemmouri scenario earthquake, however, the intensity in the western half of the Study Area is 7 to 8.
- The seismic intensity for the Sahel scenario earthquake is 8 to 9 except at EL MARSA and BORDJ EL BAHRI. The distribution pattern of seismic intensity is similar to or smaller than that of Khair al Din scenario earthquake.

- Blida scenario earthquake and Thenia scenario earthquake cause intensity 9 over a limited grid in the eastern part of the Study Area and less than 7 in the western part.
- The effect due to the Chenoua scenario earthquake is limited to AIN BENIAN with up to intensity 8.
- The estimated seismic intensity due to the Boumerdes earthquake shows intensity 8 to 9 in the eastern part of the Study Area and 6 to 7 in the western area.

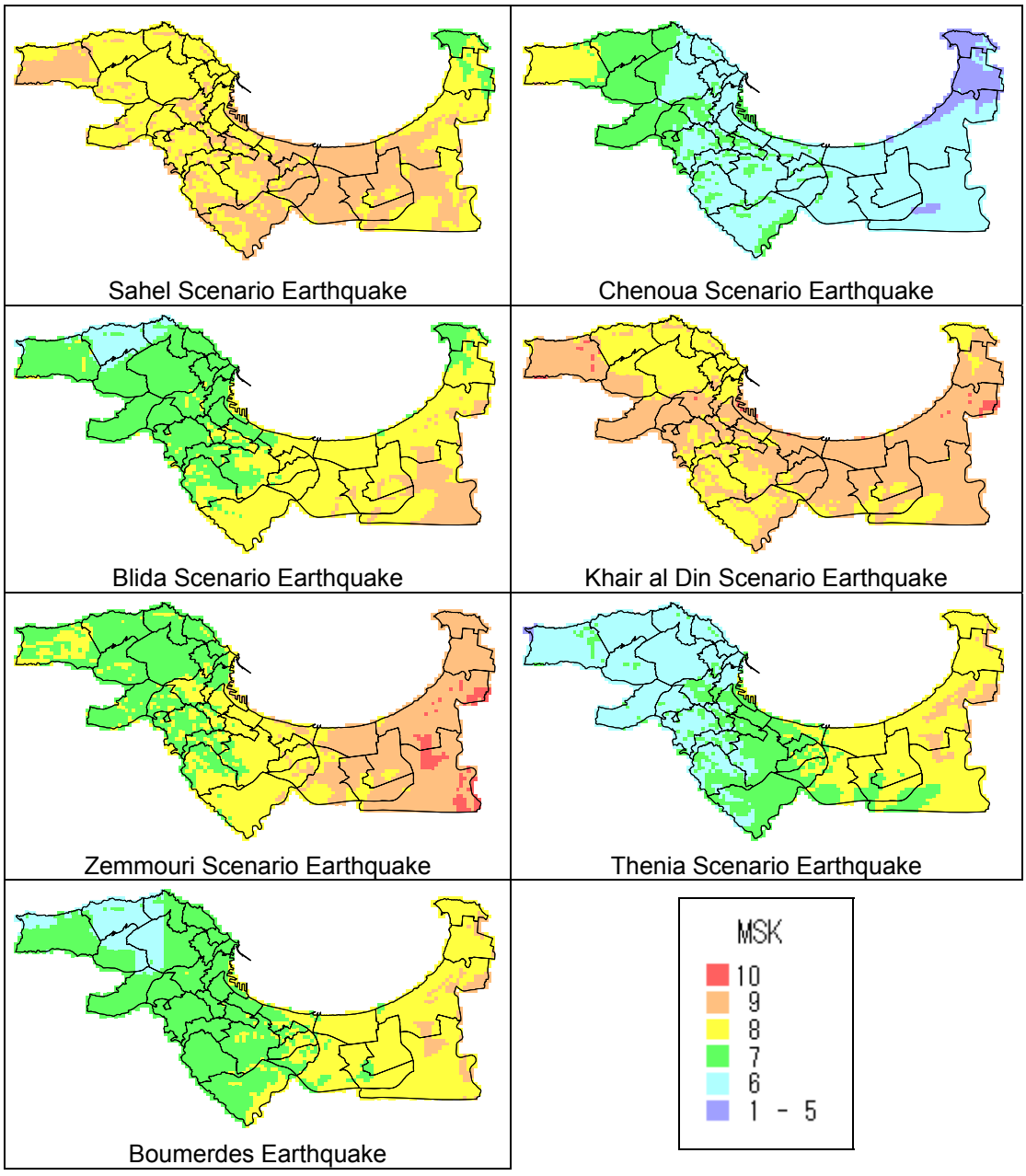

Figure 5-24 Seismic Intensity Distribution in MSK Scale

[References]
Ambraseys N.N., Douglas J., Sarma S.K. and Smit P.M., 2005, Equations for the Estimation of Strong Ground Motions from Shallow Crustal Earthquakes Using Data from Europe and the Middle East: Horizontal Peak Ground Acceleration and Spectral Acceleration. Bulletin of Earthquake Engineering, 3, pp.1-53.
Berge-Thierry, C., Cotton, F., Scotti, O., Griot-Pommera, D.-A., & Fukushima, Y., 2003, New empirical response spectral attenuation laws for moderate European earthquakes. Journal of Earthquake Engineering, 7(2), 193–222.
Delouis B., M. Vallée, M. Meghraoui, S. Calais, S. Maouche, K. Lammali, A. Mahras, P. Briole, F. Benhammouda, and K. Yelles, 2004, Slip distribution of the 2003 Boumerdes –Zemmouri earthquake, Algeria, from teleseismic, GPS, and coastal uplift data, 2004. Geoph. Res. Lett., 31, L18607, doi : 10. 1029/2004GL02687.
Laouami N., Slimani A., Bouhadad Y., and Nour A., 2005, Strong ground motions analysis of the 21st May 2003 Boumerdes (Algeria) earthquake (Mw=6.8) and elaboration of the algerian attenuation law. Submitted for publication in Soil Dynamics and Earthquake Engineering Journal.
Midorikawa S., M. Matsuoka and K. Sakugawa, 1994, Site Effects on Strong-Motion Records Observed During the 1987 Chhiba-Ken-Toho-Oki, Japan Earthquake, Proc. 9th Japan Earthq. Eng. Symp., E-085 - E-090.

5-4 Estimation of Liquefaction Potential

Land liquefaction is a phenomenon of underground water-saturated loose sand becoming liquefied at the time of an earthquake. The distribution of the sandy layer and the groundwater depth were studied at 4013 gridded area and the liquefaction potential evaluated for each. As the sandy soil was found only at the coast and along the river in the study area, the effect of liquefaction should be limited in comparison to the other hazards.

5-4-1 Methodology

(1) Analysis Procedure

Various methods have been proposed for predicting liquefaction potential. Simpler methods use the geological/geomorphological information of the study area and the relationship between geological/geomorphological units and past liquefaction behavior. If site-specific subsurface soil information is available, more detailed numerical analysis can be used. The procedure should be determined considering the objective of the analysis and the data availability. In this seismic microzoning study, soil strength and seismic motion are to be determined at uniform levels of quality for the whole study area. Therefore, using a statistical method with numerical analysis is considered appropriate.

The following information on soil properties and seismic motion was available in this study:

- Borehole logs with results of Standard Penetration Test (SPT)
- Statistically compiled physical soil properties
- Peak Ground Acceleration (PGA) for scenario earthquakes

Considering the above information, the F_L method (Japan Road Association, 2002) was adopted to estimate the liquefaction potential of the deposit at each depth. The approach of this F_L method to the assessment of liquefaction potential consists of the following steps:

1) Estimation of the liquefaction resistance of soils in a deposit (R);
2) Estimation of the shear stress likely to be induced in the soil deposit during an earthquake (L);
3) Estimation of the liquefaction potential (F_L) of the deposit, based on 1) and 2).

For the seismic microzoning purpose, it is important to estimate its effect on the ground surface or structures rather than the occurrence of liquefaction itself in the deposit. For this purpose, the liquefaction potential index P_L by Iwasaki et al. (1982) was adopted in this study. The combination of F_L method and P_L method is commonly used in Japan for practical purposes.

(2) Method of Calculation

1) F_L Method

The liquefaction potential for individual layers is analysed by the F_L method. In this study, the earthquake type to decide the parameter c_W was adopted as "Type 2" according to the seismotectonic context of the scenario earthquakes.

F_L = R/L

F_L: liquefaction resistance factor

$F_L \leq 1.0$: Judged as liquefied

$F_L > 1.0$: Judged as not liquefied

R: cyclic shear resistance at effective overburden pressure

$R = c_w \times R_L$

c_w: correlation coefficient for earthquake type

Type 1 earthquake (plate boundary type, large scale)

$c_w = 1.0$

Type 2 earthquake (inland type)

$c_w = 1.0$ $(R_L \leq 0.1)$

$= 3.3\ R_L + 0.67$ $(0.1 < R_L \leq 0.4)$

$= 2.0$ $(0.4 < R_L)$

R_L: cyclic resistance ratio obtained by laboratory test

$R_L = 0.0882\ (N_a/1.7)^{0.5}$ $(N_a<14)$

$= 0.0882(N_a/1.7)^{0.5} + 1.6\times10^{-6}(Na-14)^{4.5}$ $(14 \leq N_a)$

Sandy Soil

$N_a = c_1\ N + c_2$

$c_1 = 1$ $(0\% \leq Fc < 10\%)$

$= (Fc + 40)\ /50$ $(10\% \leq Fc < 60\%)$

$= Fc/20 - 1$ $(60\% \leq Fc)$

$c_2 = 0$ $(0\% \leq Fc < 10\%)$

$= (Fc- 10)/18$ $(10\% \leq Fc)$

Fc : fine contents (%)

Gravelly Soil

$N_a = \{1 - 0.36 \log_{10}(D_{50}/2.0)\}N_l$

N: SPT blow count

N_a: N value correlated for grain size

N_l : $170N/(\sigma_v' + 70)$

D_{50}: grain diameter of 50% passing (mm)

L: shear stress to the effective overburden pressure

$L = \alpha / g \times \sigma_v/\sigma_v' \times r_d$

r_d : stress reduction factor

$r_d = 1.0 - 0.015x$

x : depth below the ground surface (m)

α: peak ground acceleration (gal)

g: acceleration of gravity (= 980 gal)

σ_v: total overburden pressure (kN/m^2)

σ_v': effective overburden pressure (kN/m^2)

2) P_L Method

The whole liquefaction potential at each grid was evaluated by the P_L method based upon the results of the F_L method.

$$P_L = \int_0^{20} F \cdot w(z)dz$$

$15 < P_L$	Very high potential
$5 < P_L \leq 15$	Relatively high potential
$0 < P_L \leq 5$	Relatively low potential
$P_L = 0$	Very low potential

$F = 1.0 - F_L \quad (F_L < 1.0)$

$= 0.0 \quad (F_L \geq 1.0)$

$w(z) = 10.0 - 0.5z$

P_L: liquefaction potential index

F_L: liquefaction resistance factor

w(z): weight function for depth

z: depth below the ground surface (m)

5-4-2 Preconditions for the Analysis

(1) Soil Layers Studied and their Geotechnical Properties

In general, liquefaction takes place in loose alluvial saturated sandy deposits. The Japanese Design Specifications for Highway Bridges describes the following conditions for soil stratum that would require liquefaction potential evaluation:

In principle, Alluvial saturated sandy deposits, which satisfy the following three conditions at the same time, require liquefaction potential analysis:

1) Saturated sandy layer above the depth of 20 m from the present ground surface with groundwater level within 10 m from the present ground surface.
2) Soil layer with fine contents (F_C) less than 35%, or with plastic index (Ip) less than 15% even with an F_C of more than 35%.
3) Soil layer with median grain size (D_{50}) less than 10 mm, and with grain size of 10% passing less than 1 mm.

Liquefaction potential evaluation is recommended for Diluvial deposits with a low N value or without diagenesis.

The soils that require a liquefaction potential study are basically recent deposits. In this study area, "ap", "e", "a3", "a2", "q" and "qt" meet this criteria.

The necessary geotechnical properties to evaluate liquefaction potential are N value, density, D_{50}, Fc and Ip. These parameters were studied in Section 3-4 and summarized in Table 5-6. In Table 5-6, the N value is defined as a function of overburden pressure instead of unique value. Several studies reported good correlation between N value and effective overburden pressure, and the soils in Algiers also show a good correlation as shown in Figure 5-25.

Considering requirement 2) above, liquefaction is not expected if Fc is more than 35% and Ip is more than 15%, so a2 is excluded from consideration. In conclusion, the target soils are "ap", "e", "a3", "q" and "qt" in this study.

Table 5-6 Summary of Geotechnical Properties for Liquefaction Analysis

Soil	N Value [1)]	S Wave Velocity (m/sec)	Density (g/cm^3)	D_{50} (mm)	Fc (%)	Ip
ap	N=6.7P+15.5	275	1.80	0.51	16	26
e	N=6.7P+15.5 [2)]	300	1.80	0.24	11	21
a3	N=14.2P+5.1	240	1.80	0.20	23	24
a2	-	270	1.74	0.01	84	23
q	N=61.9P+5.6	300	1.81	0.42	29	23
qt	N=23.3P+15.3	330	1.90	0.15	32	24

1) P: effective overburden pressure (kgf/cm^2)
2) assumed same as "ap"

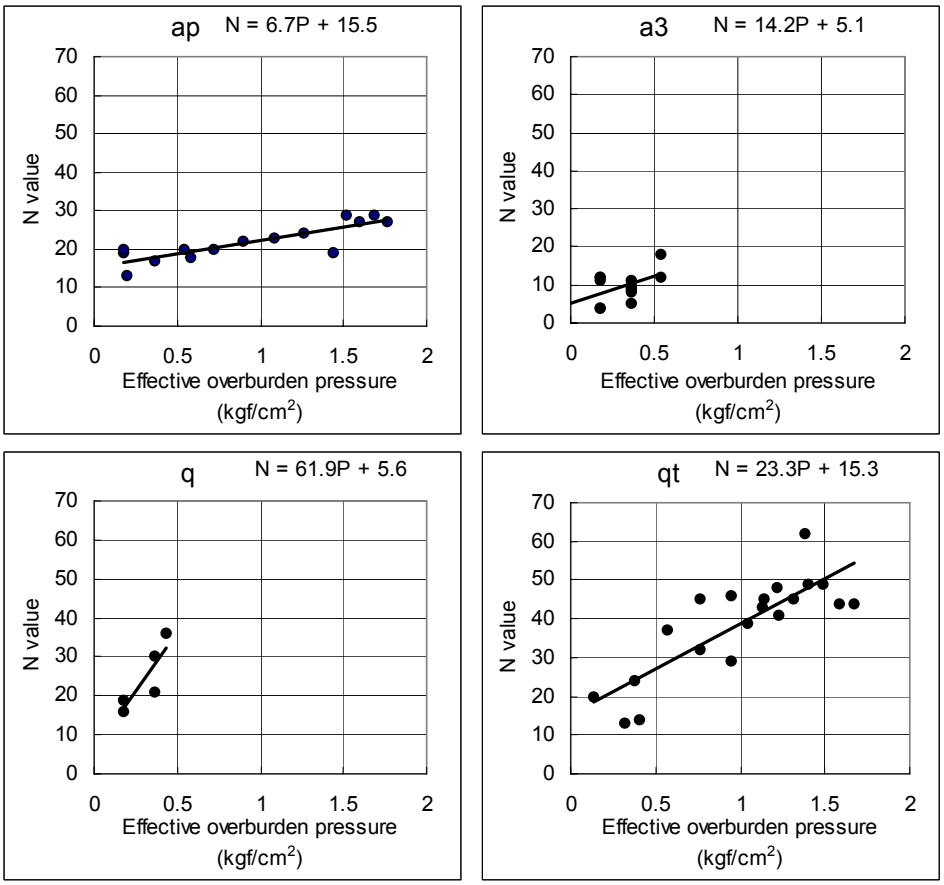

Figure 5-25 Correlation between N Value and Effective Overburden Pressure

(2) Groundwater Level

The groundwater levels of each drilling point were measured during the soil investigation in this study. The observed groundwater levels are summarized in Section 3-2-2 along with the data provided from LNHC and ANRH. Several groundwater levels show obvious discrepancy with other points because they might be the water level of a deeper aquifer rather than the surface one. The groundwater level required in the analysis of liquefaction potential is the shallowest one; therefore the groundwater level for the ground model was determined by observed data and engineering judgment.

Concerning engineering judgment, the following matters were considered:

1) The shallowest groundwater level is affected by rainfall. The soil investigation was conducted in the dry season and higher groundwater levels than observed are expected in the rainy season.

2) Several groundwater types are expected because several impermeable layers were found in the study area. Some observed / provided groundwater level data may be related to deeper aquifers, however precise interpretation is difficult.

3) The groundwater level is assumed to be shallow near the coastline or along the river. Therefore in these areas, the groundwater level was modified to be shallow. Figure 5-26 is a sample groundwater level cross-section near the Harrach River.

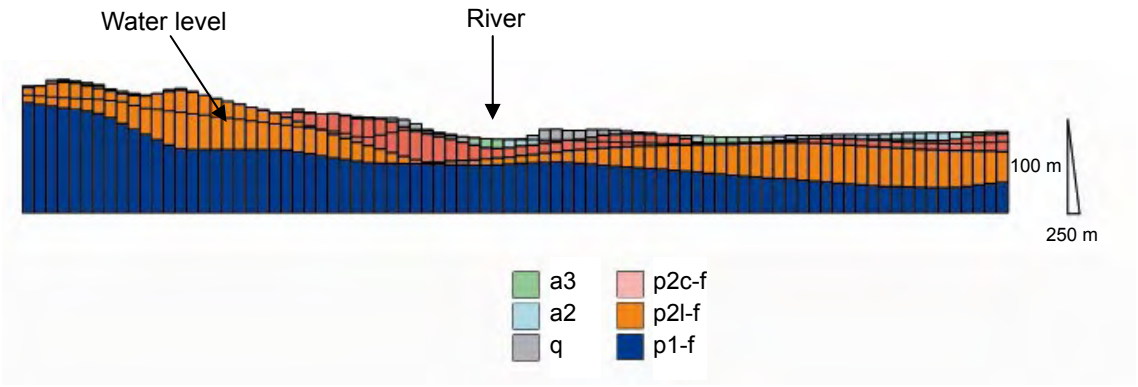

Figure 5-26 Example of Water Level Section near OUED EL HARRACH

5-4-3 Liquefaction Potential

Liquefaction potential was evaluated using P_L value (Table 5-7). The results are summarized in Figure 5-27.

The results of liquefaction analysis are described as follows:

- Boundary of EL HARRACH and BOUROUBA along OUED EL HARRACH shows high potential (shown as red color in Figure 5-27) in the Sahel scenario earthquake, Blida scenario earthquake and Khair al Din scenario earthquake.
- South-east end of BORDJ EL KIFFAN along OUED GOURER shows relatively low to high potential in Khair al Din scenario earthquake.
- South-west end of AIN BENIAN at the mouth of OUED BENI MESSOUS shows relatively low to relatively high potential in Sahel scenario earthquake and Khair al Din scenario earthquake.
- Port area shows relatively low to relatively high potential in Sahel scenario earthquake and Khair al Din scenario earthquake.

Table 5-7 Criterion for Evaluation of Liquefaction Potential

Liquefaction Potential	Criterion	Explanation
High	$15 < P_L$	Ground improvement is indispensable
Relatively High	$5 < P_L \leq 15$	Ground improvement is required Investigation of important structures is indispensable
Relatively Low	$0 < P_L \leq 5$	Investigation of important structures is required
Low	$P_L = 0$	Liquefaction prone area

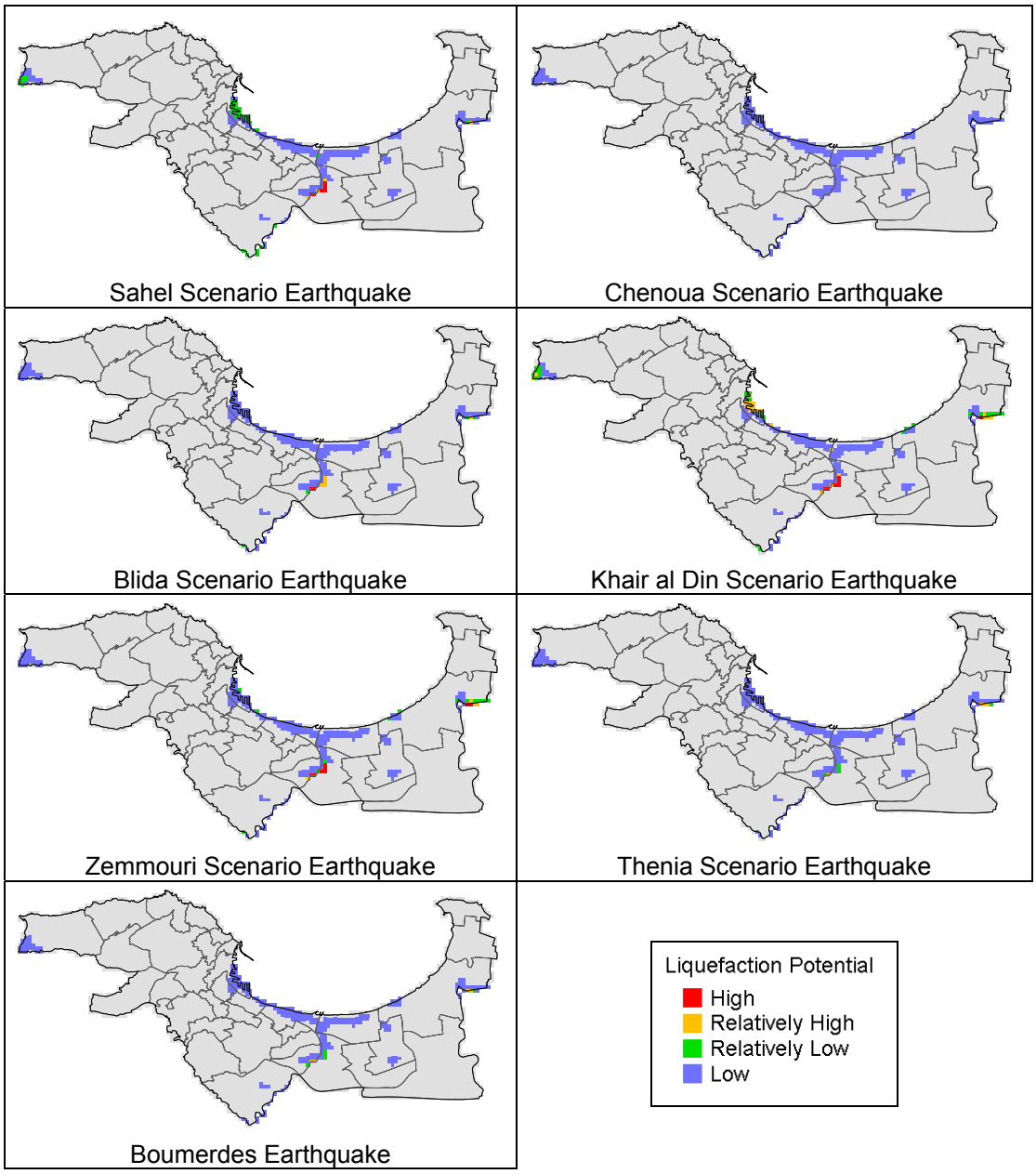

Figure 5-27 Liquefaction Potential Distribution

[References]

Iwasaki, T., Tokida, K., Tatsuoka, F., Watanabe, S., Yasuda, S. and Sato, H., 1982, Microzonation for Soil Liquefaction Potential Using Simplified Methods, Proc., 3rd Int. Conf. on Microzonation, Seattle, Vol.3, pp1319-1330.

Japan Road Association (2002). Specifications for Highway Bridges, Part V Earthquake Resistant Design.